Policy Research Working Paper 9144

Salt of the Earth

Quantifying the Impact of Water Salinity on Global Agricultural Productivity

Jason Russ
Esha Zaveri
Richard Damania
Sébastien Desbureaux
Jorge Escurra
Aude-Sophie Rodella

WORLD BANK GROUP
Water Global Practice
February 2020

Policy Research Working Paper 9144

Abstract

Salinity in surface waters is on the rise throughout much of the world. Many factors contribute to this change, including increased water extraction, poor irrigation management, and sea-level rise. To date no study has attempted to quantify the impacts on global food production. This paper develops a plausibly causal model to test the sensitivity of global and regional agricultural productivity to changes in water salinity. To do so, it utilizes several local and global data sets on water quality and agricultural productivity and a model that isolates the impact of exogenous changes in water salinity on yields. The analysis trains a machine-learning model to predict salinity globally, to simulate average global food losses over 2000–13. These losses are found to be high, in the range of the equivalent of 124 trillion kilocalories, or enough to feed more than 170 million people every day, each year. Global maps building on these results show that pockets of high losses occur on all continents, but the losses can be expected to be particularly problematic in regions already experiencing malnutrition challenges.

This paper is a product of the Water Global Practice. It is part of a larger effort by the World Bank to provide open access to its research and make a contribution to development policy discussions around the world. Policy Research Working Papers are also posted on the Web at http://www.worldbank.org/prwp. The authors may be contacted at Jruss@worldbank.org, ezaveri@worldbank.org, sebdburo@gmail.com, rdamania@worldbank.org, jorgejoseescurra@hotmail.com and arodella@worldbank.org.

Salt of the Earth: Quantifying the Impact of Water Salinity on Global Agricultural Productivity

Jason Russ, Esha Zaveri, Richard Damania, Sébastien Desbureaux, Jorge Escurra, Aude-Sophie Rodella

JEL Classification: Q10, Q11, Q15, Q25, Q53

Keywords: Agriculture, Salinity, Productivity, Food Security, Water Quality,

1. Introduction

Policy discussions surrounding agricultural water use tend to revolve around water scarcity and variability, and its impact on agricultural productivity. While these are indeed critical areas of focus, particularly in the context of climate change induced rainfall variability, challenges from water quality constitute an equally important threat that is currently underappreciated. Over-extraction of surface and groundwater, sea-water intrusion, rainfall variability, and poor irrigation water management all contribute to increased salinization of water supplies and in many regions, with deleterious effects on crop production.

Although the harm that saline soil and water can have on agricultural productivity is well known, and indeed has a long history, to date there has been no attempt to quantify this impact globally. In this paper, we take advantage of several regional and global data sets on agricultural productivity, land use, and water quality and estimate the average impact of high levels of salinity in surface water on crop production. We start with regional analyses in the Mekong River Basin and river basins of India where high-quality data exist. Using hydrological models and data on surface water irrigation, we link agricultural productivity to upstream water quality monitoring stations which indicate the levels of water salinity that is flowing onto downstream fields for irrigation. By controlling for confounding factors which also impact agricultural productivity (such as rainfall, temperature, and geographic factors), and carefully accounting for the direction of stream flow, we isolate the impact of plausibly exogenous changes in electrical conductivity (EC), the most commonly used measure of salinity in water, on downstream agricultural yields. We then expand the sample and conduct the same analysis using monitoring stations from the GEMStat database, which covers regions in 36 countries around the world.

These estimates are then used to simulate the average annual fall in yields due to saline waters. Impacts on crop production are seen at relatively low levels of salinity and tend to rise at a near linear rate as water salinity rises. A satellite-based measure of agricultural productivity, combined with estimated elasticities of agricultural yields to saline surface water, and globally modeled data on water salinity reveal significant annual losses in food production. A simulation of global food losses due to salinity is performed by training a predictive model of EC at a 0.5 degree grid between 1992 and 2013, and by combining these predictions with the elasticities we estimated. It is estimated that water salinity reduces global agricultural production by 124 trillion kilocalories per year, the equivalent annual food budget of 170 million people. These results suggest that saline surface and irrigation water are a global concern for food security that is underappreciated and deserves greater attention.

The relationship between saline water and agricultural production is well known and documented as far back as ancient Sumer (Thompson 2004). Salt can interfere with crop growth in a variety of ways; by displacing other important nutrients like nitrogen and phosphorus, interfering with photosynthesis and chlorophyll production, withdrawing water from surrounding soil, and increasing plant energy requirements for extracting water from soil (Warrence, Bauder, and Pearson 2002). Crops are not universally or uniformly impacted by salinity. Plants that have higher Na^+ and Cl^- concentrations in their leaves tend to be more salt-tolerant as it reduces the amount of salt ions that enter plant cells through osmosis (Munns and Gilliham 2015). Recently it has been estimated that approximately 1,125 million hectares of land are salt-affected, of which approximately 76 million hectares have been salinized by human-induced activities (Sanower 2019).

To our knowledge, there has been no global study attempting to estimate the impact of salinity on crop production. The literature on this topic is composed primarily of regional estimates based on crop production models or crop specific analyses which examine sensitivity to salinity for specific crops. Recent regional estimations include Dam et al. (2019), which finds that in central Vietnam, for each 1 percent increase in EC levels, yields of paddy rice decline by 0.24 percent. Clarke et al. (2015) estimate that in coastal Bangladesh, irrigating with saline surface and groundwater will reduce crop yields by at least 25 percent by the end of the century. Similarly, Dasgupta et al. (2014) estimate that rice yields will fall by 15.6 percent in by 2050 in 9 coastal districts in Bangladesh due to climate induced increases in salinity. Genua-Olmedo et al. (2016) find that in the Ebro Delta in Northeast Spain, rice productivity will fall by up to 50 percent by 2100 due to the effects of sea-level rise on soil salinity.

A deep scientific literature exists on the sensitivity of specific crops to salinity. A thorough review of this literature was conducted by Tanji and Kielen (2002) where threshold and slope values for 81 crops in terms of EC are collected and listed.[1] Similarly, Machado and Serralheiro (2017) review the literature on salt tolerance of vegetables. In table 2 they compare soil salinity and irrigation water salinity tolerance thresholds (i.e. the EC at which yields begin to decline) for 19 common vegetables. They find that vegetables generally have a soil salinity tolerance below 250 mS/m, and that irrigation water tolerances are generally around 30-50 percent less than soil salinity tolerances. Several more recent studies examine specific crops. For example, Rameshwaran et al. (2016) find that sweet peppers become sensitive to water salinity at levels exceeding 143 mS/m and decline by a slope of 11 percent thereafter. Arslan et al. (2015) found that yields of chickpeas, lentils, and fava beans fell by 50 percent when EC in irrigated water exceeded 420, 440, and 520 mS/m, respectively. This implies that based on the staple diet of countries, salinity may have an amplified impact on countries relying on agricultural production that is more salinity sensitive. While crop based studies are informative, they do not provide an indication of the global loss of food production due to salinity. To address this issue, this paper provides estimates of the average impacts on yields across all crops using a variety of recently available data sources and finds a remarkably stable yield response function that holds across wide geographies.

2. Data

To estimate the impact of water salinity on global agricultural productivity, we use several georeferenced data sets related to water quality, agricultural yields, land cover, and weather. A description of these data sets can be found below and summary statistics are provided in Table 1.

2.1 Water Quality

Data on electrical conductivity (EC) were used to measure salinity in water. EC measures the ability of an electrical charge to pass through water. Distilled, or deionized water is a very poor conductor of electricity and as dissolved ions in water increase, it becomes a better conductor. In surface and groundwaters, these ions are generally dissolved salts, which is why EC is a widely used indicator of water salinity (Miller, Bradford, and Peters 1988). EC as a measure of salinity has the added benefit of being easily measured at monitoring stations or with handheld monitors, making it a very widely available water quality indicator.

[1] See Tanji and Kielen (2002) Table A1.1 for values and list of studies.

Three distinct data sets were used to measure surface water quality. These data sets are from the Mekong River Basin Commission (MRC), the Central Water Commission (CWC) of India, and GEMStat of the United Nations Global Environmental Monitoring system for freshwater (UNGEMs). Table 2 summarizes these data sets. The MRC data span four countries (Cambodia, Lao PDR, Thailand, and Vietnam) and cover the main tributaries of the Mekong River. Of the 121 stations with data on EC, 23 are in Cambodia and Lao PDR, 21 are in Thailand, and 54 are in Vietnam (figure 1).

In India, the Central Water Commission or CWC (under the umbrella of the Ministry of Water Resources) maintains a network of 375 river monitoring stations throughout India that cover almost all major river basins in the country. Water samples are taken at specific time intervals (monthly or quarterly), and then sent to regional laboratories for analysis.

Finally, the GEMStat data from UNGEMS are used for the global analysis. These data are collected by the United National Environmental Programme (UNEP) and self-reported by participating countries. GEMStat contains over 3 million observations for 224 water quality parameters in 71 countries. EC is one of the most documented pollutants in GEMstats with 167,914 observations of EC in 1,719 stations and 71 countries. As with the Indian CWC data, frequency of observations varies significantly across countries and monitoring stations. Some monitoring stations have multiple observations per month while others have seasonal or annual observations (e.g., one station in Japan has 1,721 observations of EC only). For all the data sets, observations at a single monitoring station are collapsed at the annual level. This leaves us with a panel data set of year/station observations.

2.2 Agricultural Productivity and Land Use

To measure changes in agricultural productivity, we use a satellite-based estimate of net primary production (NPP). NPP is linearly related to the amount of solar energy that plants absorb over a growing season (Running *et al*. 2004). There is substantial evidence that there is a strong positive correlation between satellite-derived estimates of NPP and crop yields (Lobell *et al*. 2002; Lu and Zhuang, 2010; Tum and Gunther 2011), and for this reason it is a frequently used proxy of yields in the economics literature (Strobl and Strobl, 2011; Blanc and Strobl, 2013; Blanc and Strobl, 2014; Zaveri, Russ, and Damania 2019).[2]

Our time-varying NPP data come from the moderate resolution imaging spectroradiometer (MODIS), whose data start in 2000. We use the annual MOD17A3 measures from 2000-2013 generated by the Numerical Terradynamic Simulation Group (NTSG) at the University of Montana (Zhao *et al*., 2005) which corrects for cloud contamination prevalent in MODIS land products.[3]

[2] A closely related measure to NPP is the normalized difference vegetation index (NDVI). NDVI when combined with growing season data of different crops can also provide a measure of plant health and physical productivity that is directly related to NPP. For instance, MODIS-NPP is determined using NDVI along with other factors (Running et al. 2004), and in general, NDVI is considered a good predictor for NPP. However, without knowing the time-varying distribution of crops underlying the global land cover data, we cannot accurately estimate the corresponding growing season data and therefore, cannot measure the maximum NDVI during the growing season.

[3] The improved MOD17 by the NTSG is a post-reprocessed data set that corrects for cloud-contamination in NASA's MOD17 data set.

Our interest is in estimating NPP from cropland, as opposed to natural forests or vegetation. To do so, we make use of a new and unique land cover data set developed by the European Space Agency's (ESA) Climate Change Initiative. This data set provides information on 37 land cover classes based on the United Nations Land Cover Classification System at a 300m resolution. The data rely on state-of-the-art reprocessing of four different satellite missions (MERIS, SPOT-VGT, AVHRR, and PROBA-V).[4] We use a cross-walking table from Poulter *et al*. (2015) that characterizes plant functional types across the ESA classes to guide the grouping of classes into a single cropland category.[5]

Our final data measure changes in NPP for each 0.1-degree gridcell (approximately 11x11 km at the equator) which contains a minimum level of cropland in the year 2000 (the first year of our data set). There are trade-offs when choosing the minimum level of cropland for a gridcell to contain to be included the analysis. Too low of a threshold and the analysis will include gridcells which are dominated by natural vegetation or urban land, and thus of no interest to the study, potentially biasing the results. Too high of a threshold and the analysis becomes too restrictive, where only agriculture situated in large farming communities is included. For this reason, we test a range of thresholds, with the main analysis using a 30% cropland minimum threshold to be included in the analysis, and robustness checks using 75% and 90% thresholds.

2.3 Irrigation Data

Gridcells included in this analysis are restricted to those where it is believed that agriculture is irrigated. This ensures that the EC measured in the surface water is like the EC in the water which is feeding the crops. In India, data on irrigation by district were obtained from the Ministry of Agriculture and the International Crops Research Institute for the Semi-Arid Tropics. Only districts for which greater than 50 percent of agricultural land is irrigated by surface irrigation are included in the analysis (see Figure 2).

For the Mekong River basin analysis, as well as the global analysis, data on irrigation were obtained from Food and Agriculture Organization's Global Map of Irrigated Areas (GMIA) version 5.0.[6] GMIA gives a global raster of area equipped for irrigation for the year 2005 at a resolution of 0.083 degrees. These data were aggregated up to the 0.1-degree gridcell described in the previous section, and gridcells are only included if some land area is equipped for irrigation according to GMIA. GMIA does not distinguish between groundwater irrigation and surface water irrigation. For the Mekong analysis, this is not a concern, as surface water irrigation comprises 91 percent of total irrigation in Thailand, 99 percent in Lao People's Democratic Republic and Vietnam, and 100 percent in Cambodia (FAO 2016). Thus, we can be reasonably confident that nearly all the NPP included in the analysis is irrigated using surface waters.

For the wider, global study, there is unfortunately no way to distinguish between ground and surface irrigated crops. However, it is well-known that ground and surface-water bodies interact with each other. Various studies in the hydrological literature have begun to show that groundwater can be a major and potentially long-term contributor to contamination of surface water (e.g. Yu et al. 2018; Delsman et al., 2015; De Louw et al., 2010; Holman et al., 2008). The interactions between river water and

[4] https://www.esa-landcover-cci.org/.

[5] We aggregate land cover categories 10 through 30 to a single cropland class. This is also consistent with the widely-used global vegetation classification scheme of the International Geosphere Biosphere Programme (IGBP).

[6] The surface irrigation data set is available here:
http://www.fao.org/nr/water/aquastat/irrigationmap/index10.stm.

groundwater are determined by the relative difference between groundwater level and river stage (Mukherjee et al., 2018). In regions that are exposed to over-extraction of groundwater, the resulting lower discharge can reduce groundwater's contribution to the baseflow and can substantially decrease the streamflow of rivers (Mukherjee, 2018). This in turn can enhance salt concentrations in rivers because of lower dilution capacity. Excessive irrigation can also raise water tables from saline aquifers and cause seepage of saline groundwater into freshwater (Mateo-Sagasta et al., 2010).

2.4 Weather Data

Our weather data come from Matsuura and Willmott (2001). This gridded data set contains monthly observations of precipitation and average temperature at the 0.5 degree gridcell level. We transform these data into average monthly temperature, and total precipitation (mm), per year, for each gridcell.

3. Empirical Strategy

To determine the impact of saline water on crop productivity, we estimate a crop production function. Specifically, we estimate the following equation:

$$\Delta \log(NPP_{it}) = \alpha + \lambda * g(WQ_{it}) + \delta * f(climate_{it}) + \sigma_i + \rho_y + \theta_c * Y + \varepsilon_{it} \quad (1)$$

where NPP_{it} is net primary productivity in gridcell i of year t; $g(WQ_{it})$ is a measure of water quality; $f(climate_{it})$ are measures of temperature and rainfall; σ_i are gridcell fixed effects, which account for time invariant factors which impact agricultural productivity; ρ_y are year fixed effects; and $\theta_c * Y$ are region specific time trends, to account for local changes in economic or political structures which may impact agricultural production.

As discussed in the prior section, several restrictions are placed on the data set to ensure accuracy. First, only gridcells with at least 30 percent cropland according to the ESA data set are included. In robustness checks, this threshold is changed to 75 percent and 90 percent. Agriculture in gridcells must also be irrigated, as described in section 2.3. Gridcells must be no more than 100 kilometers from their matched monitoring station, to ensure that water quality at the station accurately reflects irrigation water quality. This threshold is somewhat arbitrary and chosen to balance two competing factors: higher distance thresholds reduce the average relationship between measured upstream water quality and actual water quality in the gridcell, while lower distance thresholds reduce the number of observations in our study. In section 5 we present results where this threshold is varied for robustness.

In order to avoid bias caused by reverse causality, gridcells are carefully matched to monitoring stations which are strictly upstream from them. It is well known that if drainage is not carefully managed, irrigated agriculture can impact the salinity of discharged water. Thus, downstream water salinity can be impacted by upstream agricultural production. In addition, water extractions for agriculture or other uses can also impact downstream salinity levels. Thus, to ensure that the impact of water salinity on agricultural production is properly identified and that salinity levels are entirely exogenous, a careful matching of gridcells to upstream monitoring stations was done. In the Mekong and India analyses, this was done through the use of a hydrological connectivity approach, where the streamflow from each gridcell was traced upstream until a monitoring station was found. The hydrological connectivity approach is a process in which areas of land (such as districts or grid cells) are connected to water quality stations through the drainage network based on the direction of surface runoff. To achieve this process, the following steps

were taken: (i) delineation of the drainage network of the study area; (ii) connecting the areas of land (districts in India and grid cells in the Mekong) with the drainage network; (iii) identifying the areas of land which are being impacted by the water quality stations following the drainage path; and (iv) obtaining the distance between water quality station and each of the districts and grids. For tractability, this process was changed for the global analysis. Here, given the wide geographic range of monitoring stations across the world, tracing streamflows was deemed infeasible. Thus instead, gridcells were matched to the nearest monitoring station that is at a higher elevation than the gridcell itself. Since water can only flow from higher elevations to lower elevations, this still ensures water can only flow from the monitoring station into the gridcell, and not the other way around.

4. Main Results

Beginning with the Mekong analysis, results for estimating equation 1 are shown in figure 4a. A threshold of 100 millisiemens per meter (mS/m) is used to test for impacts. This threshold is where the Mekong River Commission and other sources estimate that one should start seeing impacts on irrigated crops (Kongmeng and Larsen 2014; Tanji and Kielen 2002). The figure plots of the coefficient of the binary variable indicating observations where electrical conductivity in the upstream monitoring station exceeds 100 mS/m. Each plotted coefficient is from a different regression where the restriction on cropland within each gridcell is varied from 30 percent, 75 percent, and 90 percent. Results show that when EC exceeds 100 mS/m, there is a reduction in agricultural productivity of 5.7-8.2 percent. As the cropland requirements become more restrictive, the point estimate increases slightly, though it is not very sensitive. Figure 4b shows the similar results for the India data set. Like the Mekong region, productivity falls by 5.5-6.6 percent when EC exceeds this threshold. This threshold is exceeded by approximately 5 percent of observations in both India and the Mekong River basin. Results using the GEMStat data are shown in figure 4c. Globally, it is found that when EC exceeds 100 mS/m, yields decline by 11.0 to 13.5 percent.

Next, we estimate a more flexible model. Figure 5 shows results from creating six bins of EC, each 40mS/m wide, with the 0-40mS/m bin as the comparison group. The line graph displays the change in yields (left axis) due to a corresponding EC value shown on the x-axis. Results show a nearly linear decline in yields as EC rises. Even when EC is in the lowest bin, at 40-80 mS/m, the decline in yields is statistically detectable, and significant in magnitude at between 5.2 and 7.4 percent, relative to the omitted bin. Further, the regression is not sensitive to changing the cropland land use restriction, as all point estimates are within a tight range and all 95 percent confidence intervals overlap. The bar graphs display the percentage of observations falling into each of the buckets and correspond to the right-axis. Across all 3 samples, non-impacted observations (0-40 mS/m) represent about 50-60 percent of the sample. The next bin (40-80 mS/m) is about 30 percent of the sample, and all subsequent bins are less than 10 percent.

5. Robustness Tests

In this section we present results from two additional specifications that have been tested to corroborate the main results presented in section 4. First, we show results where we vary the distance threshold to each upstream monitoring station. Then we show results where we control for other water quality parameters in the same regression.

Here we present results from all three regional analyses for thresholds of 50km and 150km, alongside the main results. Tables 3-4 present results for the Mekong River Basin, India, and global results, respectively. In each table, results from 9 regressions are shown. The specification across all regressions are the same, with the only variation coming from the distance to monitoring station threshold and the share of cropland threshold. By changing the distance threshold, the station that each gridcell is matched to does not change, as gridcells are always matched to their nearest upstream station. Rather, what is changed is the sample of gridcells that are included in the regression, with more gridcells included as the threshold increases. Note that in each table, columns 2, 5, and 8 are the regressions depicted in 4 for cropland thresholds of 30, 75, and 90 percent, respectively. In all regions, the coefficient on EC is not sensitive to changes in the monitoring station distance threshold. Similarly, weather control variables as not sensitive as well, implying that changes to the sample to not have a significant effect on the estimates.

We next test different thresholds of high EC tested for in the Mekong River Basin and India regions. In the main results, we use 100mS/m. The true sensitivity of agriculture to EC varies by crop. The original threshold was chosen as this is the recommendation made by the Mekong River Commission and other sources as to where one should start seeing impacts on irrigated crops (Kongmeng and Larsen 2014; Tanji and Kielen 2002). However, as shown in figure 5, impacts globally are found at lower values of EC. While the Mekong River Basin and India data sets do not offer enough variation to precisely estimate a semi-parametric model like that in figure 5, we do use alternative cut offs of 75 and 125 mS/m. Results are shown in Tables 6 and 7 for the Mekong River Basin and India, respectively. In both cases, we see that impacts are found at all thresholds. In both cases, results are monotonic and scale with the threshold that is used.

6. Simulating Global Impacts of Water Salinity on Agricultural Production

The results of this paper demonstrate just how sensitive global agricultural production is to salinity in water. Using this information, we perform a simulation to quantify the magnitude of agricultural losses that saline water causes. The GEMStat database, though having wide global coverage, does not cover all land where there is agricultural production. Notably, big gaps in the data are present in China and Sub-Saharan Africa, two major agricultural areas where high salinity might be a problem (Figure 3).

To fill gaps in the GEMS data, we train a machine learning model to predict continuous values of EC globally at a 0.5-degree scale between 1992 and 2013. More specifically, we construct a data set covering the drivers of salinity identified in the scientific literature and use a Random Forest algorithm which finds the best fit between observed and predicted values over other commonly used algorithms (linear regressions, support vector machines, etc.). To estimate the model, we proceed as follows. First, we combine EC data from India, the Mekong Basin and GEMStat to have the broadest geographical coverage as possible. Second, we randomly split our data set between a training sample (80% of the observations) and a testing sample (20% of the observations). Third, we train the model on the testing sample and assess the predictive power on the testing sample. Fourth, we choose the best model as the one that maximizes the correlation coefficient between observed and predicted values in the testing sample. Finally, we use the best model to predict EC for every year between 1992 and 2013 globally at a 0.5 degree scale. More information on the covariates used and the estimation procedure can be found in Desbureaux et al (2019), which extends the approach to more parameters. The correlation coefficient between observed and predicted values of EC in the testing sample is 88 percent. Figure 6 shows the average predicted EC for each gridcell from 1992-2013. Where values are poorly predicted, the predicted EC tends to be lower than

observed EC. Consequently, the results can be interpreted as conservative predictions of the risk of high salinity.

Using the coefficients shown in figure 5 (based on 30 percent cropland), annual changes in NPP, and the EC data set described above, we estimate annual losses in agricultural productivity due to EC for each 0.5x0.5-degree gridcell where cropland exceeds 30 percent of landcover, globally. We then convert the resulting loss of NPP to kilocalorie equivalents, following Strobl and Strobl (2011) and Imhoff et al. (2014). Globally, average annual losses from 2001-2013 due to saline water total 124 trillion kilocalorie-equivalents. In total, assuming 2,000 calories/person/day, these calories represent enough food to cover the food budgets of 170 million people, annually.

The distribution of these losses is shown in Figure 7. With the exception of Sub-Saharan Africa, where most food production is rainfed, all continents have large hotspots. Very wet regions, such as the Amazon basin, Southeast Asia, and the southeastern United States also avoid losses from salinity, despite being important agricultural zones. Figure 8 aggregates losses by countries and shows further that the impact is generally not correlated with development level. The United States is the country with the largest loss of agricultural production, losing the equivalent of 32 trillion calories per year, more than double that of Argentina, the country with the next largest losses.

7. Conclusions

Addressing water quality needs for agriculture is a tremendous challenge. With agriculture responsible for 70 percent of freshwater abstractions globally, and the need for an additional 20 percent increase in water withdrawals by 2050 to feed a population of 9 billion, the problems of water scarcity often overshadow those of water quality. Nevertheless, the results in this paper demonstrate that yield losses due to saline water are significant and deserve more attention.

There is no one-size-fits-all solution to reducing salinity in irrigation waters. Solutions vary greatly by location and context. In some regions, it will require better irrigation management, to ensure that the salt balance remains low and steady. Well-designed irrigation drainage systems can accomplish this while also preventing waterlogging, which can also be harmful to crop productivity. Still, drainage systems must be carefully designed to ensure that they do not remove *too much* salt from soil layers. If draining systems do not specifically target the root layer of the soil, they may end up removing more salt from the soil than was applied by irrigation. This will cause an increase in the salt load of the water leaving the field, and impact downstream water users (Christen, Ayars, and Hornbuckle 2001).

Dealing with over-extraction is also important for reducing the occurrence of salinity in water. Over-extraction can exacerbate water salinity through reduced dilution of downstream water. Salt, at low levels of concentration, can be benign—it is only once those concentration levels become too high that productivity declines. Removing less water from the system is therefore the easiest way to prevent concentrations from becoming too high. The link between over-extraction and salinity also has the potential to lead to a vicious cycle of salinization if higher salinity levels lead to increased extraction, and therefore increased salinity. The urgency is particularly acute for countries already exposed to malnutrition and climate variability, as in the case of South Asia.

Adaptation through crop choice decisions becomes necessary when reducing salinity in water is too difficult or costly. As discussed above, crops have different tolerance levels to saline water, with some

crops experiencing large yield declines at relatively low levels of EC, and others tolerant of EC levels in excess of 1,000 mS/m. The costs and benefits of switching crop varieties, relative to other salt-mitigation strategies must be weighted at a local level to determine the best course of action for ensuring a healthy agricultural economy, as well as ensuring food security.

References

Arslan, A., Majid, G. A., Abdallah, K., Rameshwaran, P., Ragab, R., Singh, M., & Qadir, M. (2016). Evaluating the productivity potential of chickpea, lentil and faba bean under saline water irrigation systems. *Irrigation and drainage*, *65*(1), 19-28.

Blanc, E., & Strobl, E. (2013). The impact of climate change on cropland productivity: evidence from satellite based products at the river basin scale in Africa. *Climatic change*, *117*(4), 873-890.

Blanc, E., & Strobl, E. (2014). Is small better? A comparison of the effect of large and small dams on cropland productivity in South Africa. *The World Bank Economic Review*, *28*(3), 545-576.

Clarke, D., Williams, S., Jahiruddin, M., Parks, K., & Salehin, M. (2015). Projections of on-farm salinity in coastal Bangladesh. *Environmental Science: Processes & Impacts*, *17*(6), 1127-1136.

Christen, E.W., J.E. Ayars, and J.W. Hornbuckle. 2001. "Subsurface Drainage Design and Management in Irrigated Areas of Australia." *Irrigation Science* 21 (1): 35–43.

Dam, T. H. T., Amjath-Babu, T. S., Zander, P., & Müller, K. (2019). Paddy in saline water: Analysing variety-specific effects of saline water intrusion on the technical efficiency of rice production in Vietnam. *Outlook on Agriculture*, 0030727019850841.

Delsman, J. R.: Saline Groundwater – Surface Water Interaction in Coastal Lowlands, PhD thesis, VU University Amsterdam, Amsterdam, the Netherlands, 2015.

Desbureaux, S., van Vliet, M., Zaveri, E., Damania, R., Russ, J., Ribeiros, G., Rodella, A.S., and Mortier, F. (2019) *A Global Assessment of Water Quality Hotspots between 1992 and 2010 for the SDGs*.

Dasgupta, S., Hossain, M. M., Huq, M., & Wheeler, D. (2014). *Climate change, soil salinity, and the economics of high-yield rice production in coastal Bangladesh*. The World Bank.

De Louw, P. G. B., Oude Essink, G. H. P., Stuyfzand, P. J., and van der Zee, S. E. A. T. M.: Upward groundwater flow in boils as the dominant mechanism of salinization in deep polders, the Netherlands, J. Hydrol., 394, 494–506, 2010.

FAO (Food and Agriculture Organization of the United Nations). 2016. AQUASTAT Main Database, FAO, Rome. http://www.fao.org/nr/water/aquastat/data/query/index.html.

Genua-Olmedo, A., Alcaraz, C., Caiola, N., & Ibáñez, C. (2016). Sea level rise impacts on rice production: The Ebro Delta as an example. *Science of The Total Environment*, *571*, 1200-1210.

Holman, I. P., Whelan, M. J., Howden, N. J. K., Bellamy, P. H., Willby, N. J., Rivas-Casado, M., and McConvey, P.: Phosphorus in groundwater – an overlooked contributor to eutrophication, Hydrol. Process., 22, 5121–5127, 2008

Imhoff, M. L., Bounoua, L., Ricketts, T., Loucks, C., Harriss, R., & Lawrence, W. T. (2004). Global patterns in human consumption of net primary production. *Nature*, *429*(6994), 870.

Lobell, D. B., Hicke, J. A., Asner, G. P., Field, C. B., Tucker, C. J., & Los, S. O. (2002). Satellite estimates of productivity and light use efficiency in United States agriculture, 1982–98. *Global Change Biology*, *8*(8), 722-735.

Lu, X., & Zhuang, Q. (2010). Evaluating climate impacts on carbon balance of the terrestrial ecosystems in the Midwest of the United States with a process-based ecosystem model. *Mitigation and adaptation strategies for global change*, *15*(5), 467-487

Machado, R., & Serralheiro, R. (2017). Soil salinity: effect on vegetable crop growth. Management practices to prevent and mitigate soil salinization. Horticulturae, 3(2), 30.

Mateo-Sagasta, J., & Burke, J. (2011). Agriculture and water quality interactions: a global overview. SOLAW Background Thematic Report-TR08, 46.

Miller, R. L., Bradford, W. L., & Peters, N. E. (1988). *Specific conductance: theoretical considerations and application to analytical quality control*. US Government Printing Office.

Mukherjee A, Bhanja SNand Wada Y 2018 Groundwater depletion causing reduction of baseflow triggering Ganges river summer drying Sci. Rep. 8 12049

Munns, R., & Gilliham, M. (2015). Salinity tolerance of crops–what is the cost?. *New phytologist*, *208*(3), 668-673.

Poulter, B., MacBean, N., Hartley, A., Khlystova, I., Arino, O., Betts, R., ... & Hagemann, S. (2015). Plant functional type classification for earth system models: results from the European Space Agency's Land Cover Climate Change Initiative. Geoscientific Model Development, 8, 2315-2328.

Running, S. W., Nemani, R. R., Heinsch, F. A., Zhao, M., Reeves, M., & Hashimoto, H. (2004). A continuous satellite-derived measure of global terrestrial primary production. *Bioscience*, *54*(6), 547-560.

Sanower, Hossain (2019). Present Scenario of Global Salt Affected Soils, its Management and Importance of Salinity Research. International Research Journal of Biological Sciences, 1: 1-3.

Strobl E, Strobl RO (2011) The distributional impact of large dams: Evidence from cropland productivity in Africa. *Journal of Development Economics* 96(2): 432-450.

Tanji, K. K., and N. C. Kielen. 2002. *Agricultural Drainage Water Management in Arid and Semi-arid Areas.* Rome: Food and Agriculture Organization of the United Nations.

Thompson, W.R. 2004. “Complexity, Diminishing Marginal Returns, and Serial Mesopotamian Fragmentation.” *Journal of World-Systems Research* 10 (3): 613–52.

Tum, M., & Günther, K. P. (2011). Validating modelled NPP using statistical yield data. *biomass and bioenergy*, *35*(11), 4665-4674.

Warrence, N. J., Bauder, J. W., & Pearson, K. E. (2002). Basics of salinity and sodicity effects on soil physical properties. *Departement of Land Resources and Environmental Sciences, Montana State University-Bozeman, MT*, 1-29.

Yu, L., Rozemeijer, J., Van Breukelen, B. M., Ouboter, M., Van Der Vlugt, C., & Broers, H. P. (2018). Groundwater impacts on surface water quality and nutrient loads in lowland polder catchments: monitoring the greater Amsterdam area. *Hydrology & Earth System Sciences*, *22*(1).

Zaveri, E., Russ, J., & Damania, R. (2018). Drenched fields and parched farms: Evidence along the extensive and intensive margins. *Available at SSRN 3104224*.

Zhao, M., Heinsch, F. A., Nemani, R. R., & Running, S. W. (2005). Improvements of the MODIS terrestrial gross and net primary production global data set. *Remote sensing of Environment*, *95*(2), 164-176.

Figures

Figure 1- Mekong River Basin Commission Monitoring Station Locations

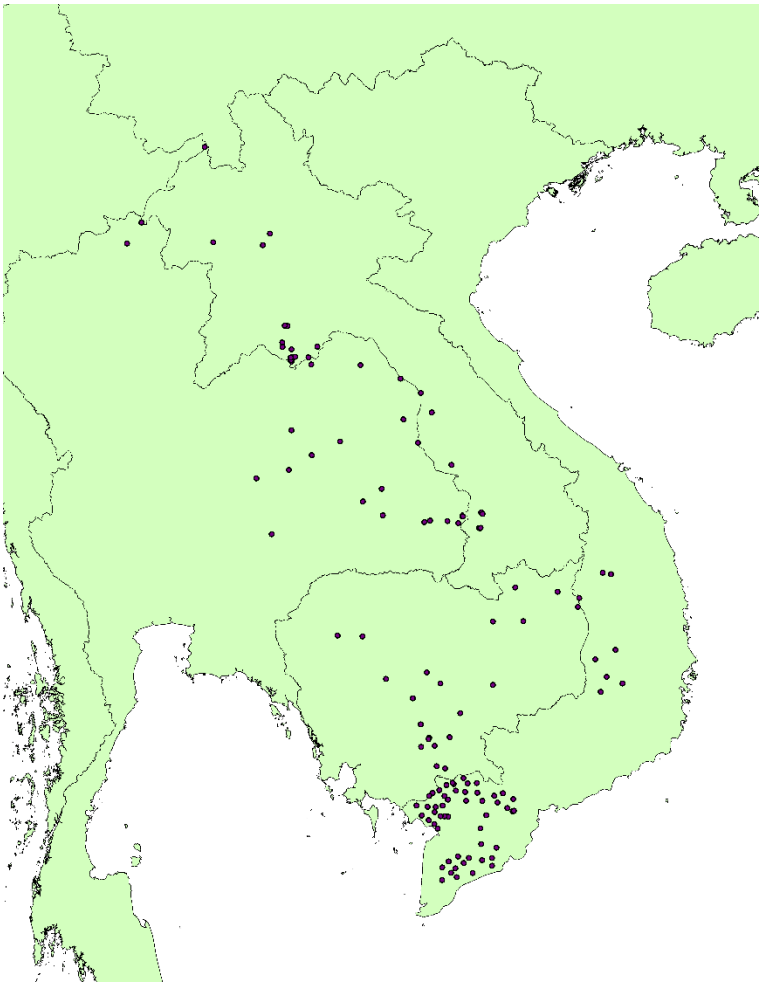

Notes: Map shows location of water quality monitoring stations in Mekong River Basin Commission data set.

Figure 2: CWC monitoring stations and irrigated districts in India

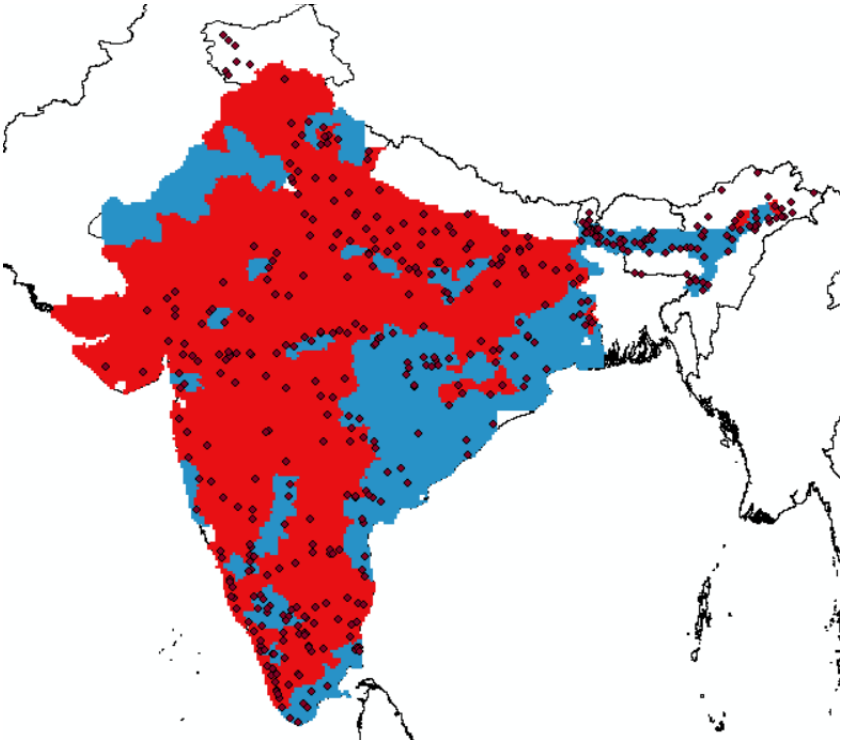

Notes: Figure shows districts in blue where at least 50 percent of agriculture is irrigated using surface irrigation. Black dots show the location of the CWC monitoring stations.

Figure 3: Location of GEMStat monitoring stations

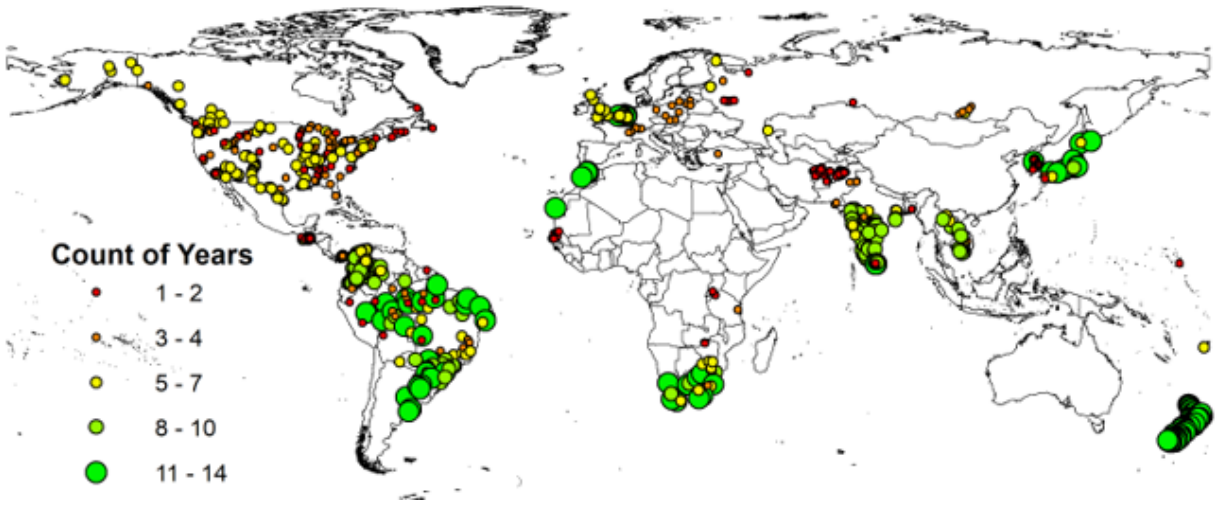

Notes: Figure shows the location of GEMStat monitoring stations with data on EC from 2000-2013. The size and color of the dots denotes the number of years for which there is EC data at each station during this time period

Figure 4: Yield loss when electrical conductivity exceeds 100mS/m

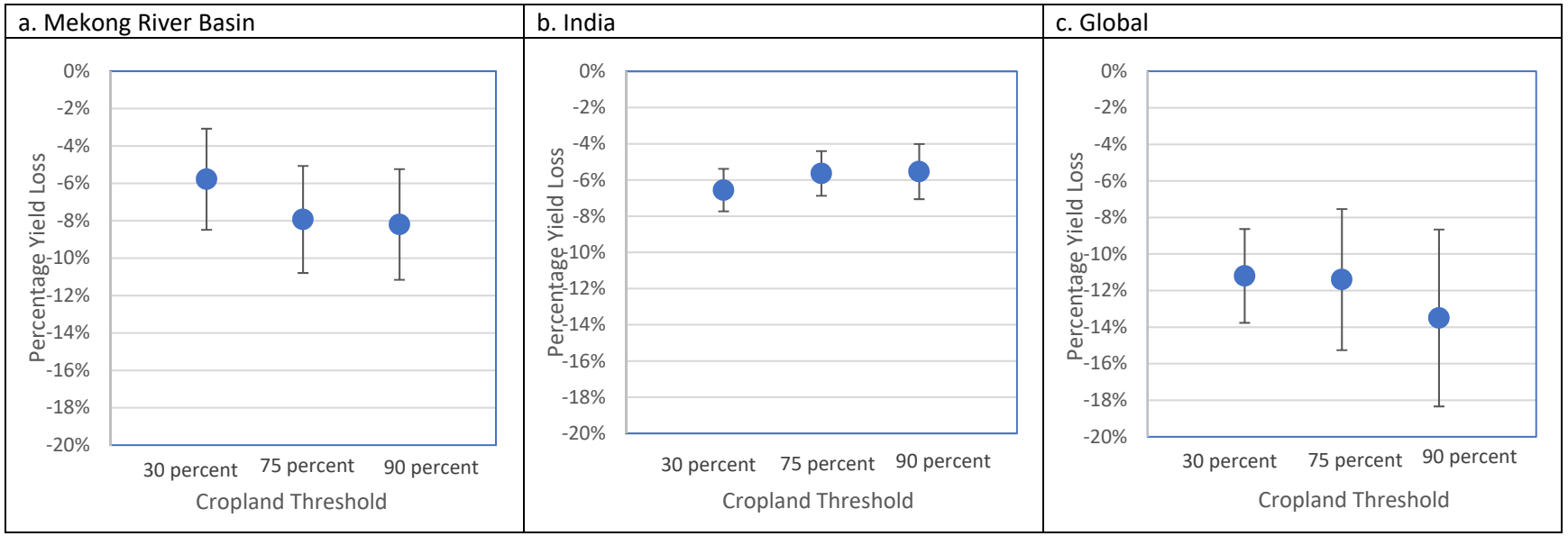

Notes: Figure shows results from estimating equation 1 in 3 different regions. Figure a (left) if in the Mekong River Basin, figure b (center) is in India, and figure c (right) is global using GEMStat data. In each region, coefficients from three different regressions are shown. The three regressions vary the restrictions on the share of cropland within a gridcell needed to be included in the regression. The left estimate includes all gridcells with at least 30 percent cropland in the year 2000. The mid and right estimate include gridcells with at least 75 percent and 90 percent cropland, respectively. The point estimate shown is the coefficient on a binary variable indicating observations where electrical conductivity in the upstream monitoring station exceeds 100mS/m. Error bars show the 95 percent confidence interval based on standard errors clustered at the gridcell level.

Figure 5: Flexible estimation of yield losses due to electrical conductivity

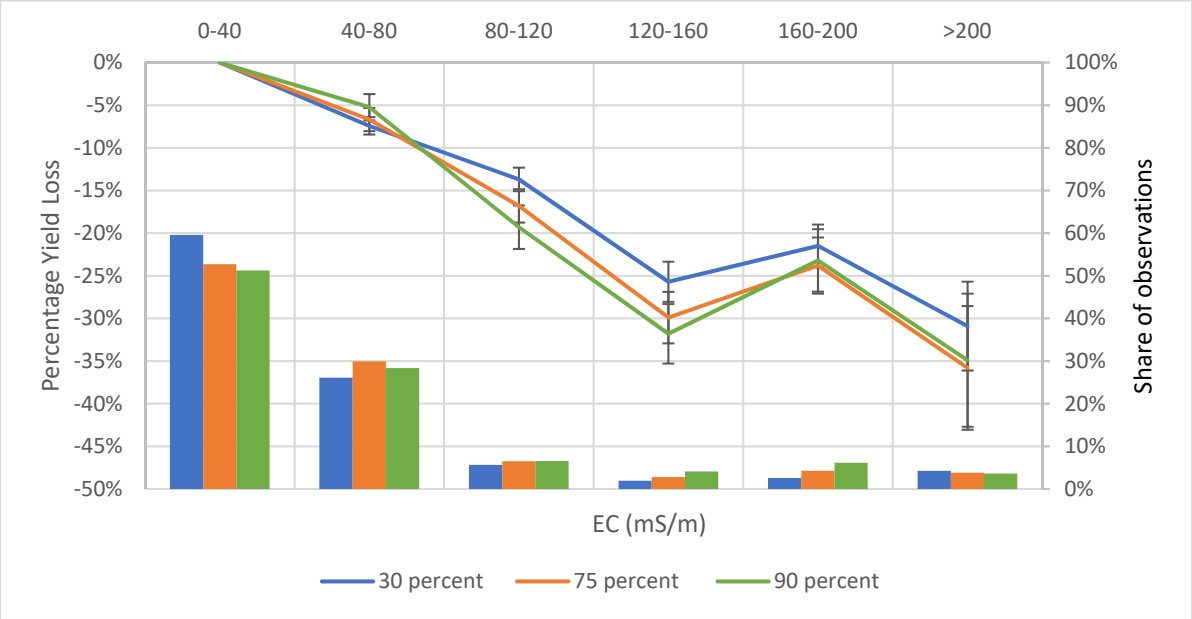

Notes: Figure shows results from estimating equation 1 using water quality data from GEMStat. The three regressions vary the restrictions on the share of cropland within a gridcell needed to be included in the regression. The blue line includes all gridcells with at least 30 percent cropland in the year 2000. The red and green lines include gridcells with at least 75 percent and 90 percent cropland, respectively. The point estimate shown is the coefficient on an indicator variable which indicates if EC is within the range given on the x-axis. Error bars show the 95 percent confidence interval based on standard errors clustered at the gridcell level.

Figure 6: Global Predicted Levels of EC, 1992-2010

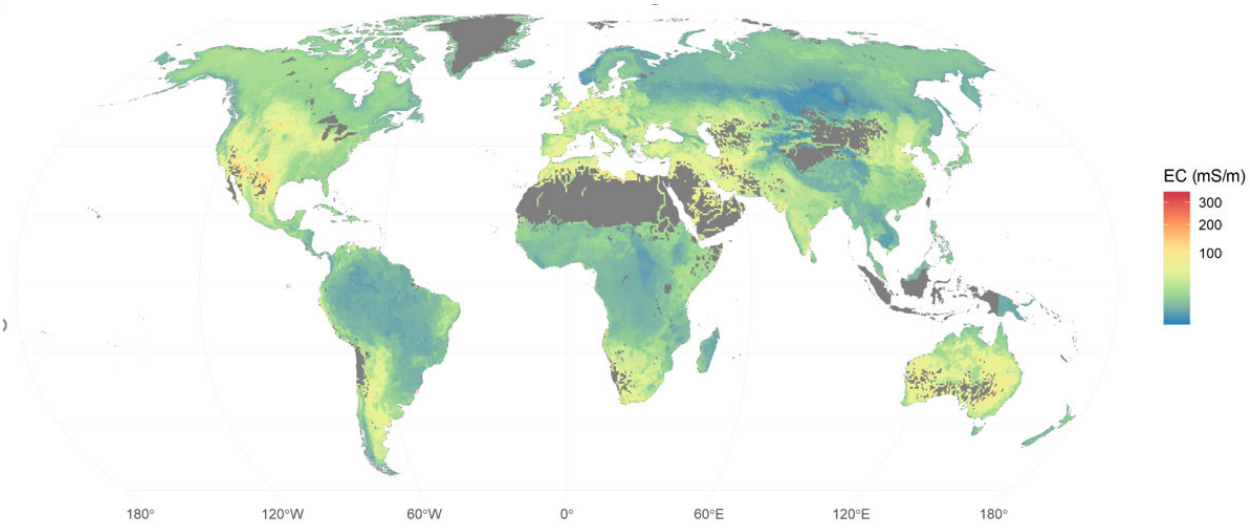

Notes: Figure shows average predicted EC from 1992-2010 for each gridcell from Désbureaux et al (2019)

Figure 7: Estimated Mean Annual Kilocalorie Equivalent Loss due to Saline Water, 2001-2013

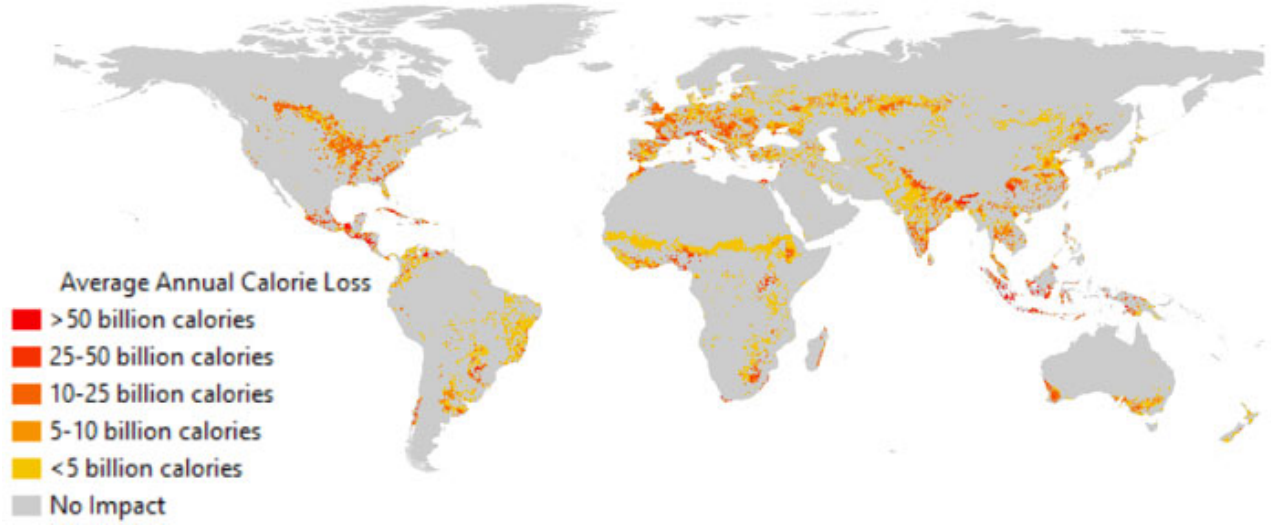

Notes: Figure shows estimated average annual kilocalorie equivalent losses across space for the years 2001-2013. Losses are estimated based on the coefficients in 5, predicted EC from Désbureaux et al (2019) and net primary productivity data from Zhao et al., 2005.

Figure 8: Estimated Mean Losses in Agricultural Production due to Saline Water, 2001-2013, by Country

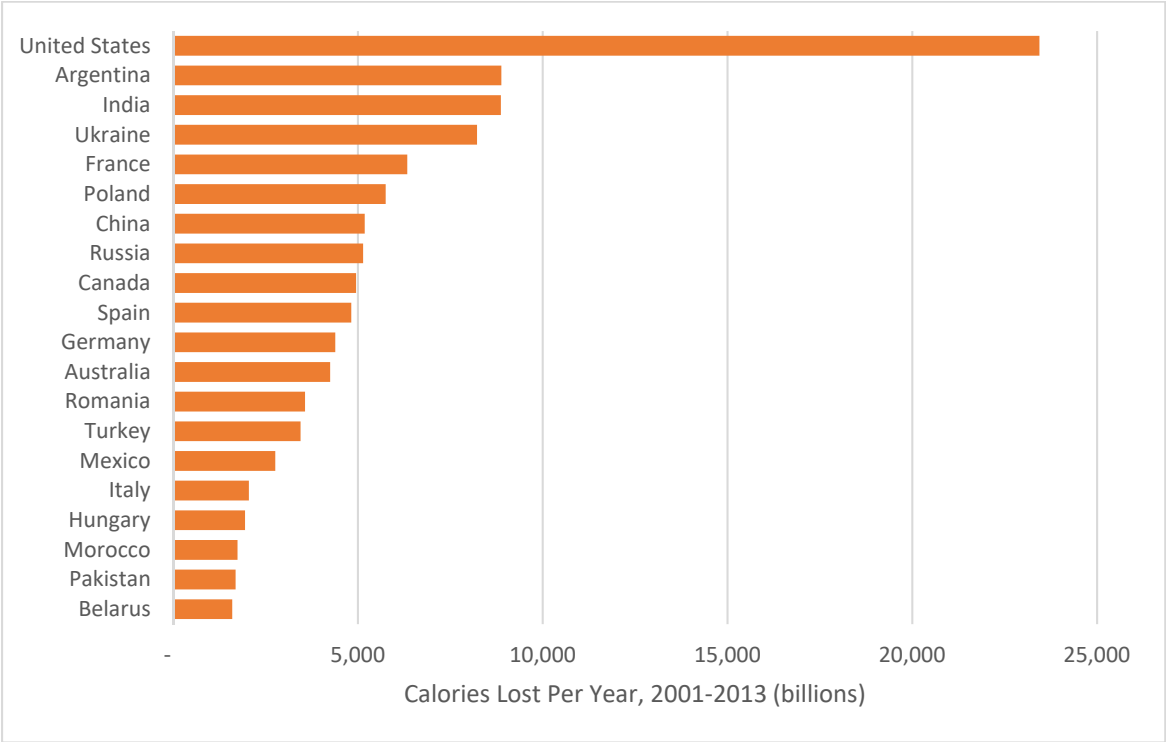

Notes: Figure aggregates estimated average annual losses based on the country which the centroid of each gridcell lies.

Tables

Table 1: Summary Statistics of Major Data Sets

Variable	Obs	Mean	Std. Dev.	Min	Max
		Mekong River Basin			
Δlog(NPP)	3227	-0.00256	0.146958	-0.52872	0.573803
Electricial Conductivity	3784	127.8139	442.9442	3.2	3598.75
Electrical Conductivity > 100 mS/m	3784	0.075317	0.263937	0	1
Precipitation (m/year)	3784	1.545724	0.423054	0.4649	3.0135
Precipitation^2 (m/year)	3784	2.56819	1.433598	0.216132	9.081182
Temperature (C)	3784	27.31999	1.070222	21.225	29.70833
Temperature^2 (C)	3784	747.5272	57.06304	450.5006	882.5851
Distance to station (km)	3784	40.70026	23.44734	1.501745	99.66087
		India			
Δlog(NPP)	23,786	0.022225	0.281151	-2.70913	3.197244
Electricial Conductivity	26,830	405.1288	311.6987	48.43333	2230
Electrical Conductivity > 100 mS/m	26,830	0.061014	0.23936	0	1
Precipitation (m/year)	26,830	1.156739	0.59924	0.1696	4.8393
Precipitation^2 (m/year)	26,830	1.697122	2.267632	0.028764	23.41882
Temperature (C)	26,830	26.36198	1.755244	15.13333	29.66667
Temperature^2 (C)	26,830	698.0349	90.26891	229.0178	880.1112
Distance to station (km)	26,830	54.64403	24.02906	0.783259	99.94202
		Global			
Δlog(NPP)	55,358	0.014986	0.276158	-3.8473	4.766428
Electricial Conductivity	68,984	596.4569	1666.453	0	41914.29
Electrical Conductivity > 100 mS/m	68,984	0.100792	0.301055	0	1
Precipitation (m/year)	68,984	1.199992	0.657942	0.0005	5.1165
Precipitation^2 (m/year)	68,984	1.872862	2.244765	0.00	26.17857
Temperature (C)	68,984	21.59153	6.87379	2.333333	31.1
Temperature^2 (C)	68,984	513.4423	267.854	5.444445	967.21
Distance to station (km)	68,984	50801.36	29429.34	0	99997.37

Notes: Table summarizes the main data sets use in each of the three models employed in this paper.

Table 2: Water Quality Data Sets

Location	**Mekong River Basin (Cambodia, Lao PDR, Thailand, and Vietnam)**	**India**	**Global (36 countries)**
Source	Mekong River Basin Commission	Central Water Commission for India	GEMStat
Number of Monitoring Stations Included	121	425	1,124
Frequency of Observations	Approximately monthly, with gaps	Varies by station	Varies by station
Years of Observations	2000-2013	2000-2013	2000-2013

Table 3: Impact of Electrical Conductivity on Net Primary Productivity, Mekong River Basin

Dep Var: Δ log(net primary productivity)	(1)	(2)	(3)	(4)	(5)	(6)	(7)	(8)	(9)
Electrical Conductivity > 100 mS/m	-0.0550 (0.0138)***	-0.0578 (0.0138)***	-0.0605 (0.0137)***	-0.0764 (0.0149)***	-0.0793 (0.0146)***	-0.0834 (0.0140)***	-0.0801 (0.0163)***	-0.0820 (0.0151)***	-0.0851 (0.0143)***
Precipitation (m/year)	-0.207 (0.0282)***	-0.202 (0.0236)***	-0.204 (0.0226)***	-0.182 (0.0352)***	-0.199 (0.0293)***	-0.200 (0.0282)***	-0.196 (0.0469)***	-0.234 (0.0404)***	-0.240 (0.0387)***
Precipitation^2 (m/year)	0.0519 (0.00783)***	0.0508 (0.00667)***	0.0501 (0.00647)***	0.0427 (0.00964)***	0.0461 (0.00799)***	0.0452 (0.00782)***	0.0433 (0.0132)**	0.0513 (0.0112)***	0.0521 (0.0108)***
Temperature (C)	0.268 (0.0826)**	0.223 (0.0628)***	0.175 (0.0572)**	0.131 (0.116)	0.109 (0.0966)	0.0949 (0.0889)	0.117 (0.149)	0.138 (0.121)	0.166 (0.111)
Temperature^2 (C)	-0.00437 (0.00153)**	-0.00352 (0.00116)**	-0.00260 (0.00106)*	-0.00187 (0.00213)	-0.00144 (0.00177)	-0.00112 (0.00163)	-0.00160 (0.00271)	-0.00199 (0.00220)	-0.00248 (0.00203)
Year Fixed Effects	Y	Y	Y	Y	Y	Y	Y	Y	Y
Gridcell Fixed Effects	Y	Y	Y	Y	Y	Y	Y	Y	Y
Geographic Time Trends	Country	Country	Country	Country	Country	Country	Country	Country	Country
Distance to nearest station	50km	100km	150km	50km	100km	150km	50km	100km	150km
Cropland Threshold	>30%	>30%	>30%	>75%	>75%	>75%	>90%	>90%	>90%
N	2623	3784	4367	1746	2576	2986	1224	1821	2144
R-sq	0.647	0.674	0.689	0.610	0.645	0.657	0.588	0.620	0.630

Notes: Table shows results from estimating equation 1 for the Mekong River Basin sample via ordinary least squares. Each column is from a separate regression. Specifications across regressions remain constant, with only the sample of gridcells included differing. Columns 1-3 include gridcells where land area is at least 30 percent cropland. Columns 4-6 restrict the sample to gridcells to those with at least 75 percent cropland, and columns 7-9 restrict to sample to gridcells with at least 90 percent cropland. Gridcells are also restricted based on the distance to the nearest upstream monitoring station. Columns 1, 4, and 7 include gridcells less than 50km from the nearest upstream station, columns 2, 5, and 8 include gridcells less than 100km from the nearest upstream station, and columns 3, 7, and 9 include gridcells less than 150km from the nearest upstream station. Standard errors clustered at the gridcell level are in parentheses. Stars denote level of statistical significance: + p<0.1, * p<0.05, ** p<0.01, *** p<0.001

Table 4: Impact of Electrical Conductivity on Net Primary Productivity, India

Dep Var: Δ log(net primary productivity)	(1)	(2)	(3)	(4)	(5)	(6)	(7)	(8)	(9)
Electrical Conductivity > 100 mS/m	-0.0968 (0.0095)***	-0.0656 (0.0060)***	-0.0651 (0.0047)***	-0.103 (0.0107)***	-0.0564 (0.00634)***	-0.0558 (0.00505)***	-0.121 (0.0143)***	-0.0554 (0.00777)***	-0.0532 (0.0061)***
Precipitation (m/year)	0.310 (0.03)***	0.325 (0.02)***	0.346 (0.02)***	0.372 (0.04)***	0.334 (0.03)***	0.351 (0.0248)***	0.402 (0.06)***	0.347 (0.03)***	0.353 (0.03)***
Precipitation^2 (m/year)	-0.0706 (0.00853)***	-0.0776 (0.0068)***	-0.0881 (0.0063)***	-0.104 (0.0147)***	-0.0911 (0.00962)***	-0.102 (0.00857)***	-0.111 (0.0203)***	-0.0924 (0.0123)***	-0.102 (0.0113)***
Temperature (C)	-0.494 (0.0927)***	-0.407 (0.0592)***	-0.327 (0.0529)***	-0.715 (0.110)***	-0.599 (0.0701)***	-0.506 (0.0632)***	-0.762 (0.130)***	-0.724 (0.0829)***	-0.663 (0.0755)***
Temperature^2 (C)	0.00740 (0.00176)***	0.00563 (0.00114)***	0.00403 (0.00102)***	0.0113 (0.00209)***	0.00892 (0.00135)***	0.00711 (0.00122)***	0.0125 (0.00245)***	0.0115 (0.00159)***	0.0102 (0.00145)***
Year Fixed Effects	Y	Y	Y	Y	Y	Y	Y	Y	Y
Gridcell Fixed Effects	Y	Y	Y	Y	Y	Y	Y	Y	Y
Geographic Time Trends	State	State	State	State	State	State	State	State	State
Distance to nearest station	50km	100km	150km	50km	100km	150km	50km	100km	150km
Cropland Threshold	>30%	>30%	>30%	>75%	>75%	>75%	>90%	>90%	>90%
N	11655	26830	35074	8720	20663	26865	6516	15698	20558
R-sq	0.473	0.476	0.474	0.469	0.478	0.474	0.463	0.467	0.471

Notes: Table shows results from estimating equation 1 for the India sample via ordinary least squares. Each column is from a separate regression. Specifications across regressions remain constant, with only the sample of gridcells included differing. Columns 1-3 include gridcells where land area is at least 30 percent cropland. Columns 4-6 restrict the sample to gridcells to those with at least 75 percent cropland, and columns 7-9 restrict to sample to gridcells with at least 90 percent cropland. Gridcells are also restricted based on the distance to the nearest upstream monitoring station. Columns 1, 4, and 7 include gridcells less than 50km from the nearest upstream station, columns 2, 5, and 8 include gridcells less than 100km from the nearest upstream station, and columns 3, 7, and 9 include gridcells less than 150km from the nearest upstream station. Standard errors clustered at the gridcell level are in parentheses. Stars denote level of statistical significance: + $p<0.1$, * $p<0.05$, ** $p<0.01$, *** $p<0.001$

Table 5: Impact of Electrical Conductivity on Net Primary Productivity, Global

Dep Var: Δ log(net primary productivity)	(1)	(2)	(3)	(4)	(5)	(6)	(7)	(8)	(9)
Electrical Conductivity > 100 mS/m	-0.0917***	-0.112***	-0.112***	-0.0814***	-0.114***	-0.114***	-0.116***	-0.135***	-0.135***
	(0.0156)	(0.0131)	(0.0131)	(0.0224)	(0.0197)	(0.0197)	(0.0304)	(0.0247)	-0.0247
Precipitation (m/year)	0.568***	0.552***	0.552***	0.834***	0.777***	0.777***	1.14***	0.992***	0.992***
	(0.03)	(0.02)	(0.02)	(0.06)	(0.04)	(0.04)	(0.09)	(0.06)	(0.06)
Precipitation^2 (m/year)	-0.117***	-0.114***	-0.114***	-0.221***	-0.206***	-0.206***	-0.345***	-0.308***	-0.308***
	(0.00714)	(0.00501)	(0.00501)	(0.0211)	(0.0147)	(0.0147)	(0.0329)	(0.0200)	-0.02
Temperature (C)	0.121***	0.141***	0.141***	0.219***	0.222***	0.222***	0.359***	0.292***	0.292***
	(0.0103)	(0.00744)	(0.00744)	(0.0187)	(0.0128)	(0.0128)	(0.0413)	(0.0245)	-0.0245
Temperature^2 (C)	-0.00337***	-0.00420***	-0.00420***	-0.00570***	-0.00609***	-0.00609***	-0.00866***	-0.00758***	-0.00758***
	(0.000276)	(0.000199)	(0.000199)	(0.000500)	(0.000326)	(0.000326)	(0.000929)	(0.000543)	-0.000543
Year Fixed Effects	Y	Y	Y	Y	Y	Y	Y	Y	Y
Gridcell Fixed Effects	Y	Y	Y	Y	Y	Y	Y	Y	Y
Geographic Time Trends	State	State	State	State	State	State	State	State	State
Distance to nearest station	50km	100km	150km	50km	100km	150km	50km	100km	150km
Cropland Threshold	>30%	>30%	>30%	>75%	>75%	>75%	>90%	>90%	>90%
N	33236	68984	68984	16550	35070	35070	9110	20002	20002
R-sq	0.243	0.237	0.237	0.281	0.275	0.275	0.325	0.314	0.314

Notes: Table shows results from estimating equation 1 for the global sample using the GEMStat database via ordinary least squares. Each column is from a separate regression. Specifications across regressions remain constant, with only the sample of gridcells included differing. Columns 1-3 include gridcells where land area is at least 30 percent cropland. Columns 4-6 restrict the sample to gridcells to those with at least 75 percent cropland, and columns 7-9 restrict to sample to gridcells with at least 90 percent cropland. Gridcells are also restricted based on the distance to the nearest upstream monitoring station. Columns 1, 4, and 7 include gridcells less than 50km from the nearest upstream station, columns 2, 5, and 8 include gridcells less than 100km from the nearest upstream station, and columns 3, 7, and 9 include gridcells less than 150km from the nearest upstream station. Standard errors clustered at the gridcell level are in parentheses. Stars denote level of statistical significance: + p<0.1, * p<0.05, ** p<0.01, *** p<0.001

Table 6: Impact of Electrical Conductivity on Net Primary Productivity, alternative thresholds, Mekong River Basin

	(1)	(2)	(3)
Dep Var: Δ log(net primary productivity)	EC > 75ms/m	EC > 100ms/m	EC > 125ms/m
Electrical Conductivity exceeds threshold	-0.0409	-0.0578	-0.0578
	(0.0125)**	(0.0138)***	(0.0138)***
Precipitation (m/year)	-0.201	-0.202	-0.202
	(0.0236)***	(0.0236)***	(0.0236)***
Precipitation^2 (m/year)	0.0507	0.0508	0.0508
	(0.00668)***	(0.00667)***	(0.00667)***
Temperature (C)	0.224	0.223	0.223
	(0.0628)***	(0.0628)***	(0.0628)***
Temperature^2 (C)	-0.00353	-0.00352	-0.00352
	(0.00116)**	(0.00116)**	(0.00116)**
Year Fixed Effects	Y	Y	Y
Gridcell Fixed Effects	Y	Y	Y
Geographic Time Trends	Country	Country	Country
Distance to nearest station	50km	50km	50km
Cropland Threshold	>30%	>30%	>30%
N	3784	3784	3784
R-sq	0.674	0.674	0.674

Notes: Table shows results from estimating equation 1 for the Mekong River Basin sample via ordinary least squares. Each column is from a separate regression, and regressions vary by the threshold of EC used in the EC indicator variable. Standard errors clustered at the gridcell level are in parentheses. Stars denote level of statistical significance: + p<0.1, * p<0.05, ** p<0.01, *** p<0.001

Table 7: Impact of Electrical Conductivity on Net Primary Productivity, alternative thresholds, India

	(1)	(2)	(3)
Dep Var: Δ log(net primary productivity)	EC > 75 mS/m	EC > 100 mS/m	EC > 125 mS/m
Electrical Conductivity exceeds threshold	-0.0315	-0.0656	-0.0752
	(0.00477)***	(0.00600)***	(0.0102) ***
Precipitation (m/year)	0.329	0.325	0.326
	(0.0212)***	(0.0212)***	(0.0212)***
Precipitation^2 (m/year)	-0.0779	-0.0776	-0.0771
	(0.00682)***	(0.00682)***	(0.00679)***
Temperature (C)	-0.419	-0.407	-0.392
	(0.0590)***	(0.0592)***	(0.0585)***
Temperature^2 (C)	0.00587	0.00563	0.00540
	(0.00113)***	(0.00114)***	(0.00112)***
Year Fixed Effects	Y	Y	Y
Gridcell Fixed Effects	Y	Y	Y
Geographic Time Trends	State	State	State
Distance to nearest station	100km	100km	100km
Cropland Threshold	>30%	>30%	>30%
N	26830	26830	26830
R-sq	0.475	0.476	0.476

Notes: Table shows results from estimating equation 1 for the India sample via ordinary least squares. Each column is from a separate regression, and regressions vary by the threshold of EC used in the EC indicator variable. Standard errors clustered at the gridcell level are in parentheses. Stars denote level of statistical significance: + $p<0.1$, * $p<0.05$, ** $p<0.01$, *** $p<0.001$